

PERMEABILITY, TORTUOSITY, AND ATTENUATION OF WAVES IN POROUS MATERIALS¹

Krzysztof Wilmanski
Berlin

The paper contains a consistent presentation of the construction of a linear poroelastic model and its applications in the theory of acoustic waves. The main purpose of this presentation is the discussion of material parameters describing the diffusion. This concerns particularly the permeability and tortuosity. In Section 2 we mention a few examples of porous systems in which diffusion processes play an important role. Section 3 contains a concise description of the two-component model describing saturated porous materials with diffusion. We point out the main features of such a system with the special emphasis of relative motion of components and changes of porosity. As a special case the governing equations of Biot's model are presented. In Section 4 we discuss the notions of permeability, hydraulic conductivity and tortuosity. In particular the notion of the tortuosity tensor is introduced. Section 5 is the primer of the nuclear magnetic resonance method of experimental determination of permeability and tortuosity in various porous materials. Finally, Section 6 contains some issues concerning the propagation of monochromatic waves and, in particular, an influence of tortuosity on speeds and attenuation.

Key words: porous media, diffusion, permeability, tortuosity, acoustic waves

1. INTRODUCTION

The most important feature which distinguishes porous materials from composites is the possibility of diffusion. Obviously, such materials as closed

¹ A part of this Article was presented at the IIIrd Conference: *Mechanics of Inhomogeneous Media*, Lagow, 4-6 June 2010 under the title: "*Tortuosity of porous media and its influence on properties of acoustic waves* (in Polish).

cell foams or perforated plates seem to belong to the class of porous materials. However, the way in which they are modeled as continua, i.e. smearing out procedures is for such systems identical as those for standard composites. This is not the case when cavities are connected with each other as in open cell foams. A fluid component or components filling these cavities may move independently of the motion of the skeleton (i.e. of the solid phase). Such diffusion processes are always connected with the dissipation, i.e. they are irreversible processes. Intensity of dissipation depends on relative velocities of components and on material properties of the porous medium. It was Henry Philibert Gaspard Darcy (born 10 June 1803 in Dijon and died on 3 January 1858) who proposed a linear law relating the pressure gradient (or hydraulic gradient) with the filtration (i.e. relative) velocity or discharge of the fluid through a unit surface. A coefficient in this law – the permeability – is strongly dependent on properties of both skeleton and a fluid, on the geometry of channels and on the geometry of the flow (tortuosity).

In this work, we present a motivation for theoretical continuous modeling of diffusion in porous materials. Some prominent examples of practically important processes are presented in the next Section of the paper. We indicate there some references where phenomenological details and a microscopical background can be found.

In Section 3 we present a continuous model of saturated porous materials. We limit the attention to processes with a small deformation of the skeleton and of the fluid component. This yields the linearity of the model with respect to the changes of geometry and, consequently, it is convenient to use the Eulerian description of motion. However, we indicate certain nonlinear contributions connected with the diffusion. In the macroscopic description the fluid component is inviscid. The real fluid is viscous and this leads to the momentum source in partial balance equations which is defined by a convolution integral. This type of relation was suggested by M.A. Biot [19, 20] and it yields for monochromatic acoustic waves a dependence of the permeability on the frequency. In Section 4 we elaborate the structure of the momentum source which is the most essential part of the model of diffusion.

Numerous material parameters appearing in the theoretical model can be either estimated theoretically by means of averaging procedures or by measurements. We shall not present the former problem and refer to original papers on the subject (e.g. [85]). However, we do go into some details of experimental techniques which deliver data characterizing diffusion. These are, in particular, methods based on the nuclear magnetic resonance (NMR). In Section 5, we present a primer of the physical background for these techniques, demonstrate some measuring devices and some results of experiments on porous materials.

Section 6 is devoted to some properties of monochromatic acoustic waves in saturated porous materials. These results form the foundation for some nondestructive methods of observation of porous materials. We discuss in some details the structure of governing equations following within the model presented in Section 3 and, in particular, an influence of the so-called added mass effect. This has been related by J. G. Berryman *et al.* [17], D. L. Johnson *et al.* [46] and some others to the tortuosity. We show that this relation is a pure artifact following from a mistake made in the paper [46].

2. DIFFUSION IN VARIOUS SYSTEMS

Diffusion may be a spontaneous process in natural systems such as soils or it may be forced for some practical purposes such as filtration. Some most prominent examples of systems in which the diffusion is important are as follows.

A: Fuel cells [37]. Fuel cells differ from usual electric batteries in this respect that they are open to the environment. In a typical fuel cell, a fuel is continuously fed to the anode and an oxidant (e.g. oxygen from air) is continuously fed to the cathode. In principle, fuel cells produce power as long as a fuel is supplied. In Fig.1, a schematic of the polymer electrolyte membrane fuel cell (PEMFC [53]) is shown where the oxidation of hydrogen produces the electric current.

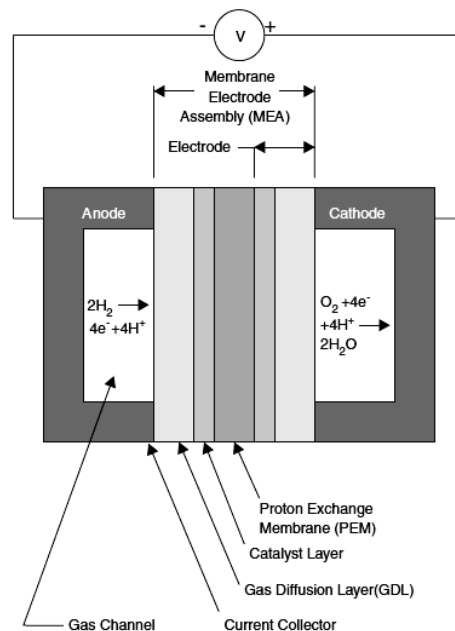


Fig. 1. Schematic of PEM fuel cell

The main problem in design and theoretical modeling of such systems is a correct balance of transport processes. These transport processes enhance the delivery of oxygen to the catalyst layer and appropriate removal of water from the electrode. It means that the water which is produced in the synthesis should not be removed too rapidly as this would lead to drying of electrodes and it would reduce the performance of the cell. This indicates that diffusion processes in such systems must be very carefully calculated and controlled.

B. Soils and rocks. These are two different types of materials: the former is made of loose or loosely connected mesoparticles such as grains or platelets while the latter consists of a solid skeleton with voids and channels. In spite of this fundamental difference both diffusion and heat conduction processes can be described for both types by a similar model. Obviously, diffusion processes play a different role in those materials. In the second case, they are primarily related to the transport of fluids and, in the case of freezing of water in pores, may influence rates and extent of damage processes. In the first case, they may directly yield substantial changes of mechanical properties. For instance, when dry, clays become firm and fired in kilns transform to ceramics. Sands may suffer structural instabilities due to the diffusion such as liquefaction. Such a process accompanying an earthquake is schematically shown in Fig. 2.

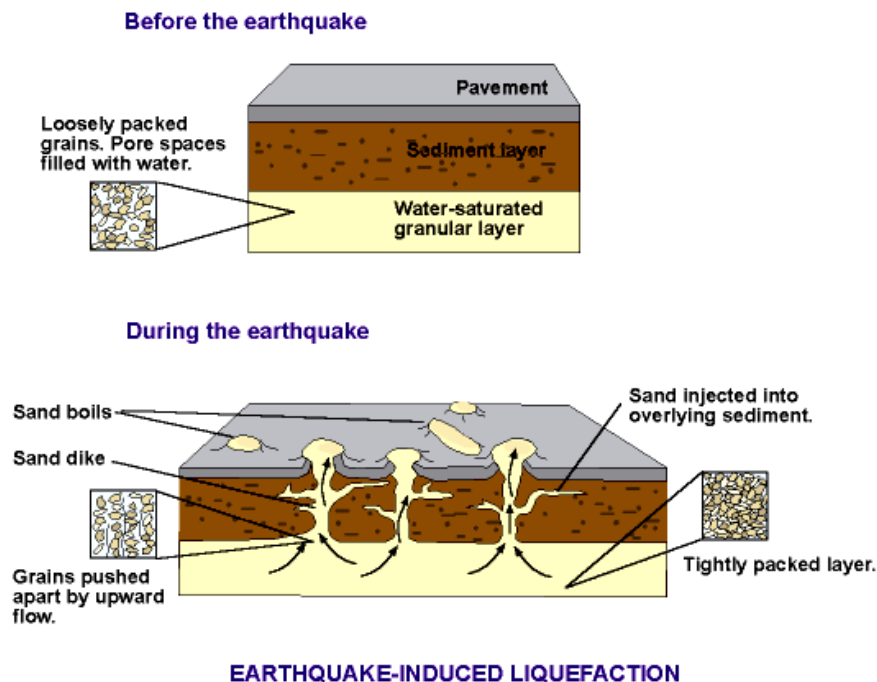


Fig. 2. Diffusion in sand during the earthquake causing the liquefaction

C. Tissues, in particular brain. All living tissues are porous and they “live” due to diffusion processes. These may proceed on a microscopic level and then molecules diffuse through membranes or they may appear on mesoscopic level in which case the diffusion appears in channels of porous materials. Such is the motion of air in bronchi and lungs and the motion of fluids in the brain.

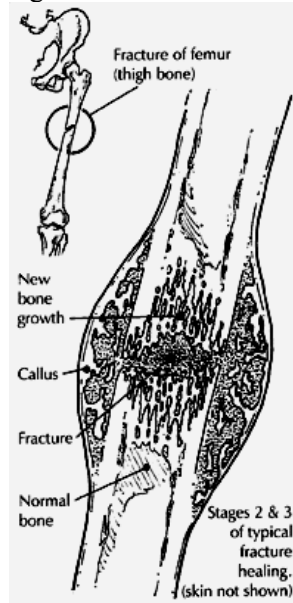


Fig. 3. Healing of the fractured bone

In Fig. 3, we show a fractured bone which heals by producing collagen fibers in the processes of local diffusion. Its rate depends on the level of stresses in the vicinity of fracture and on permeability properties of tissues involved in the healing process. Such a problem of fracture healing was, for instance, theoretically investigated in the paper [35].

Fig. 4 demonstrates a typical picture of the brain structure obtained by the method of diffusion nuclear magnetic imaging. We return later to the presentation of this nondestructive testing method which plays a very important role not only in medicine but also in chemistry, mechanics of porous materials, geotechnics, etc. These pictures show an anisotropy of the white matter tracts in brain conducting fluids. This anisotropy results from the fibrous structure of neural axons. Water is transported easier in the direction of these fibers and this gives rise to the graphical representations of the white matter of the brain called tractography. Results of such imaging yield important conclusions on pathology of the brain such as schizophrenia (e.g. [74]) or location of tumors. Similar methods are applied in the diagnosis of pathological changes of muscles, for instance, in the heart. Based on a multicomponent model of diffusion are

attempts to describe the growth and spread of tumors (see [29] for further references).

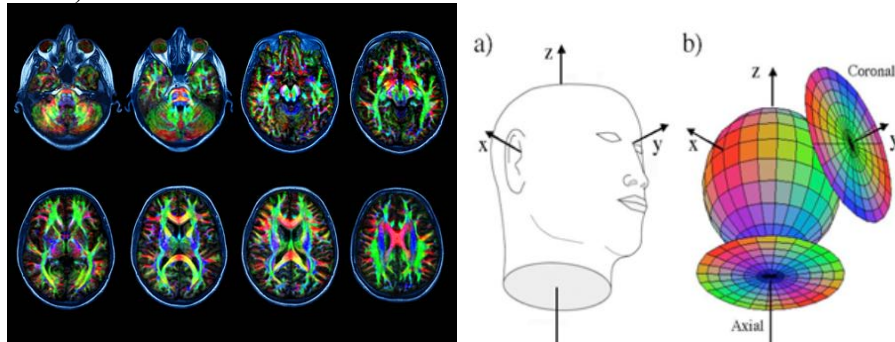


Fig. 4. Diffusion MRI pictures of brain demonstrating an anisotropy of permeability. The right figure prescribes colors to directions [65]

D. Filters and transport of pollutants. Filters are porous materials in which diffusion processes are coupled with processes of adsorption (e.g. [1, 14, 15, 38, 83]), i.e. attraction of molecules (adhesion or cohesion) from a fluid mixture flowing through the material by surfaces of channels.



Fig. 5: Pollen car filter eliminating dust and other particles from incoming air

In Fig. 5, we show a typical pollen filter appearing in all modern cars which adsorbs dust from the inflowing air. Similar filters are applied in air conditioners. Many types of porous microfilters are applied in pharmacy, biology and other branches where the separation of substances with molecules of

different size from a suspension is necessary. Natural processes of filtration and contaminant transport appear in soils and sand filters.

E. Crystal growth by sublimation. Diffusion processes play an important role in all techniques of the growth of single crystals. In two most popular methods of floating zone (FZ) and Czochralski (CZ) these are surface processes. In growth by sublimation the diffusion through a volume of the porous material (porous graphite and granular silicium) play an important role (compare: [27, 28, 60]).

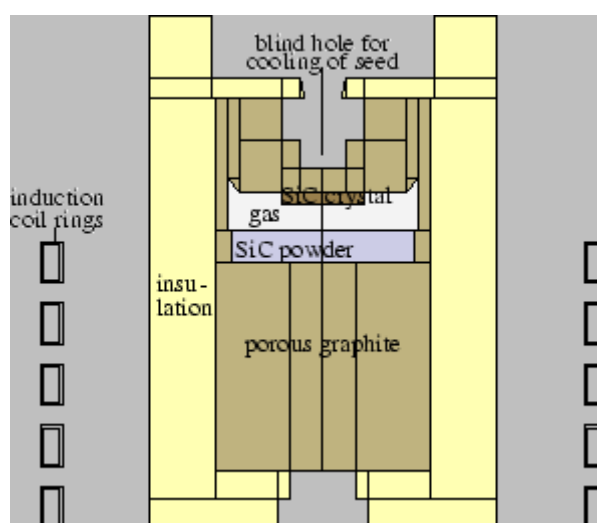


Fig.6. Schematic of the growth of SiC single crystals by sublimation

In Fig. 6, we show a schematic of a growth chamber for SiC crystals in which the porous zones are indicated.

3. THEORETICAL MODELS OF A SATURATED POROUS MEDIUM

Theoretical macroscopic description of diffusion processes is often based on a simplified model in which deformations of components are neglected. This means that the skeleton is assumed to be rigid and the fluid is incompressible. Then the mass conservation of the fluid component and the so-called Darcy law yield a parabolic diffusion equation. Such a model is sufficient in many practical problems of filtration or ground water motion. However, many diffusion processes are coupled with deformations of the skeleton (e.g. lungs), deformations of the fluid (e.g. flow of gases through porous materials). In any case, these couplings are essential in the description of acoustic properties of porous materials. We proceed to present a simple model of such coupled processes.

A saturated porous medium consists of two components: a solid skeleton and a fluid in the pores. If we neglect the mass exchange between these two components such a system can be modeled as an immiscible mixture [76, 88]. Then we have to formulate field equations for the following quantities

$$\{\rho^S, \rho^F, n, \mathbf{v}^S, \mathbf{v}^F, \mathbf{e}^S\}, \quad (1)$$

where ρ^S, ρ^F are current mass densities of the skeleton and of the fluid, respectively, n denotes current porosity, $\mathbf{v}^S = v_i^S \mathbf{e}_i$, $\mathbf{v}^F = v_i^F \mathbf{e}_i$ are macroscopic (average) velocities of both components and $\mathbf{e}^S = e_{ij}^S \mathbf{e}_i \otimes \mathbf{e}_j$ is the Almansi-Hamel measure of small deformations of the skeleton. Obviously, $\mathbf{e}_i, i=1,2,3$, $\mathbf{e}_i \cdot \mathbf{e}_j = \delta_{ij}$, denote the base vectors of the Cartesian frame of reference. Further, we use only such frames. As we have already mentioned, one can construct a nonlinear model in which deformations are large and processes are not isothermal. Then the set of fields (1) must contain the temperature and the motion of the skeleton must be described by a function of motion in the Lagrangian description. Such a model has been constructed (e.g. see [88]) but we do not discuss it in this work.

The linearity of the model with respect to deformations means that we make the following assumption

$$\begin{aligned} \|\mathbf{e}^S\| \ll 1, \quad |\varepsilon| \ll 1, \\ (\mathbf{e}^S - \lambda^{(\alpha)} \mathbf{1}) \mathbf{n}^{(\alpha)} = \mathbf{0}, \quad \alpha = 1,2,3, \quad \|\mathbf{e}^S\| = \max |\lambda^{(\alpha)}|, \\ \varepsilon = \frac{\rho_0^F - \rho^F}{\rho_0^F}, \end{aligned} \quad (2)$$

where $\lambda^{(\alpha)}$ are the eigenvalues of the deformation tensor \mathbf{e}^S (principal stretches), $\mathbf{n}^{(\alpha)}$ are eigenvectors (principal directions) of the deformation of the skeleton and ε denotes volume changes of the fluid for small deformations. In this work, we denote by the index 0 the initial constant value of the corresponding quantity. In the above relations ρ_0^F is the initial value of the partial mass density of the fluid. Certainly, volume changes of the skeleton in the linear theory are given by the relation

$$e = \text{tr} \mathbf{e}^S = \sum_{\alpha=1}^3 \lambda^{(\alpha)}. \quad (3)$$

It should be kept in mind that all these fields are defined on a common macroscopic domain \mathcal{B} and therefore they differ from real mesoscopic quantities such as real (true) mass density of the skeleton or the fluid, ρ^{SR}, ρ^{FR} or from real (true) velocities of the skeleton and the fluid, $\mathbf{v}^{SR}, \mathbf{v}^{FR}$. We return later to this problem.

Governing equations for the fields (1) follow from partial balance equations of mass and momentum. We use here, as everywhere else in this paper the Eulerian description. They have the form

$$\begin{aligned} \frac{\partial \rho^S}{\partial t} + \rho_0^S \operatorname{div} \mathbf{v}^S &= 0, & \frac{\partial \rho^F}{\partial t} + \rho_0^F \operatorname{div} \mathbf{v}^F &= 0, \\ \rho_0^S \frac{\partial \mathbf{v}^S}{\partial t} &= \operatorname{div} \mathbf{T}^S + \hat{\mathbf{p}}^S + \rho_0^S \mathbf{b}^S, \\ \rho_0^F \frac{\partial \mathbf{v}^F}{\partial t} &= \operatorname{div} \mathbf{T}^F + \hat{\mathbf{p}}^F + \rho_0^F \mathbf{b}^F, \end{aligned} \quad (4)$$

while the balance equation of porosity has the form [82, 88]:

$$\frac{\partial \Delta_n}{\partial t} + \Phi_0 \operatorname{div} (\mathbf{v}^F - \mathbf{v}^S) = \hat{n}, \quad \Delta_n = n - n_E. \quad (5)$$

We neglect mass sources and nonlinear kinematic contributions. $\mathbf{T}^S = \sigma_{ij}^S \mathbf{e}_i \otimes \mathbf{e}_j$, $\mathbf{T}^F = \sigma_{ij}^F \mathbf{e}_i \otimes \mathbf{e}_j$ denote partial stress tensors. As we assume the fluid component to be inviscid on the macroscopical level we have

$$\mathbf{T}^F = -p^F \mathbf{1} \quad \text{i.e.} \quad \sigma_{kk}^F = -3p^F, \quad (6)$$

where p^F is the partial pressure in the fluid. $\hat{\mathbf{p}}^S, \hat{\mathbf{p}}^F$ are momentum sources and they satisfy the momentum conservation law

$$\hat{\mathbf{p}}^S = -\hat{\mathbf{p}}^F. \quad (7)$$

$\mathbf{b}^S, \mathbf{b}^F$ are the densities of partial body forces. They may include contributions following from a noninertial frame of reference, such as centrifugal, Coriolis and Euler forces.

The quantity n_E , appearing in the porosity balance equation is the so-called equilibrium porosity and \hat{n} is the source of porosity. We return later to the discussion of these notions. The equation (5) was introduced by K. Wilmanski [82] and, in a simplified form - without porosity source - it appears

also in the book of T. J. T. Spanos [71] (eqn. (2.87)) and – without diffusion but with the source – in the works of R. M. Bowen (e.g. [26], eqn. (5A.4.11)).

In the equation (5), Φ_0 is a material constant defining the flux of porosity for isotropic materials. In the case of anisotropic materials, it would be a tensor of the second rank, $\Phi_0 = \Phi_{ij} \mathbf{e}_i \otimes \mathbf{e}_j$, but we shall not discuss this kind of anisotropy in this work.

In addition to balance equations, the deformation tensor of the skeleton must satisfy the usual integrability condition of the continuum which in the linear theory has the following form

$$\frac{\partial \mathbf{e}^S}{\partial t} = \text{sym grad } \mathbf{v}^S \quad \Rightarrow \quad \frac{\partial e}{\partial t} = \text{div } \mathbf{v}^S. \quad (8)$$

The second equation, according to the relation (3), describes volume changes of the skeleton.

For poroelastic materials the second law of thermodynamics yields fairly explicit constitutive relations which are needed for the following quantities

$$\{\mathbf{T}^S, p^F, \hat{\mathbf{p}}^S, n_E, \hat{n}\} \quad (9)$$

For isotropic materials they have the following form [86, 87]

$$\begin{aligned} \mathbf{T}^S &= \mathbf{T}_0^S + \lambda^S e \mathbf{1} + 2\mu^S \mathbf{e}^S + Q\varepsilon \mathbf{1} + \beta(n - n_E) \mathbf{1} - N(n - n_0) \mathbf{1}, \\ p^F &= p_0^F - Qe - \rho_0^F \kappa \varepsilon + \beta(n - n_E) + N(n - n_0), \\ \hat{\mathbf{p}}^S &= -\hat{\mathbf{p}}^F = \pi * (\mathbf{v}^F - \mathbf{v}^S), \\ n_E &= n_0(1 + \delta e), \end{aligned} \quad (10)$$

where the momentum source is given by the convolution integral

$$\begin{aligned} \pi * (\mathbf{v}^F - \mathbf{v}^S) &= \\ &= \pi(0)(\mathbf{v}^F(t) - \mathbf{v}^S(t)) + \int_0^\infty \frac{d\pi}{ds}(s) [\mathbf{v}^F(t-s) - \mathbf{v}^S(t-s)] ds. \end{aligned} \quad (11)$$

We discuss this relation further in some details.

It should be mentioned that the influence of the nonequilibrium deviation of porosity described by the material parameter β (the underlined terms in (10)) is negligible in the wave analysis [3].

The source of porosity $\hat{\mathbf{p}}^S$ may contain an additional term describing the influence of the relative acceleration. Such a contribution was introduced by M. A. Biot [20] and it was attributed to an influence of tortuosity [17, 25, 45, 46]. It

has been shown [86] that such a linear contribution is not objective (frame-dependent) but it can be corrected in a nonlinear way to be objective. Then it has the form

$$\hat{\mathbf{a}}_r = \frac{\partial}{\partial t}(\mathbf{v}^F - \mathbf{v}^S) + (\mathbf{v}^S \cdot \text{grad})(\mathbf{v}^F - \mathbf{v}^S) - (1 - \zeta) \left((\mathbf{v}^F - \mathbf{v}^S) \cdot \text{grad} \right) \mathbf{v}^F - \zeta \left((\mathbf{v}^F - \mathbf{v}^S) \cdot \text{grad} \right) \mathbf{v}^S, \quad (12)$$

where ζ is the material parameter. Obviously, in the linear approximation there remains only the difference of time derivatives (the underlined term) and this alone is not objective. If we include this dependence on the relative acceleration, the momentum source becomes

$$\hat{\mathbf{p}}^S = \pi * (\mathbf{v}^F - \mathbf{v}^S) - \rho_{12} \mathbf{a}_r, \quad (13)$$

where the material coefficient ρ_{12} is sometimes interpreted as an influence of the so-called added mass effect. This effect appears in the description of resistance forces for flows of fluids around obstacles (e.g. [63]). We shall discuss this issue in the Section on the waves.

In addition, a thermodynamic analysis shows that such an extension of the momentum source yields as well the correction of constitutive relations for stresses [86, 89]

$$\begin{aligned} \mathbf{T}^S = \mathbf{T}^S &= \mathbf{T}_0^S + \lambda^S e \mathbf{1} + 2\mu^S \mathbf{e}^S + Q\varepsilon \mathbf{1} + \beta(n - n_E) \mathbf{1} - \\ &\quad - N(n - n_0) \mathbf{1} - \underline{\underline{\zeta \rho_{12} (\mathbf{v}^F - \mathbf{v}^S) \otimes (\mathbf{v}^F - \mathbf{v}^S)}}, \\ p^F &= p_0^F - Qe - \rho_0^F \kappa \varepsilon + \beta(n - n_E) + \\ &\quad + N(n - n_0) + \underline{\underline{\frac{1}{3}(1 - \zeta) \rho_{12} (\mathbf{v}^F - \mathbf{v}^S) \cdot (\mathbf{v}^F - \mathbf{v}^S)}}}. \end{aligned} \quad (14)$$

Obviously, the double underlined terms are nonlinear. However, it should be mentioned that, in contrast to the first term in (13), the contribution of relative accelerations does not yield an additional dissipation in the system (for details see: [86]). For isothermal processes and without porosity source, $\hat{n} = 0$, this is defined by the relation

$$\mathcal{D} = (\mathbf{v}^F - \mathbf{v}^S) \cdot [\pi * (\mathbf{v}^F - \mathbf{v}^S)] \geq 0, \quad (15)$$

which means that a selection of material parameters ρ_{12}, ζ does not influence the dissipation. Such an influence may be possible in highly nonlinear models of dissipation processes which goes beyond the contemporary nonequilibrium thermodynamics and, most likely, has no practical bearing.

The constitutive relations (10) specify the so-called Biot model of saturated porous materials, commonly used in acoustics of such materials. Such a model follows from the above relations if we leave out nonlinear contributions (the double underlined terms in (14)) and assume in addition

$$\beta = 0, \quad N = 0, \quad \hat{n} = 0. \quad (16)$$

Lack of sources of porosity allows to integrate the balance equation of porosity (5). We obtain

$$n = n_0 \left(1 + \delta e + \frac{\Phi_0}{n_0} (\varepsilon - e) \right), \quad (17)$$

where the following relations, resulting from partial mass balance equations, have been used

$$\begin{aligned} \frac{\partial e}{\partial t} &= \operatorname{div} \mathbf{v}^S, & \frac{\partial \varepsilon}{\partial t} &= \operatorname{div} \mathbf{v}^F, \\ e &= \frac{\rho_0^S - \rho^S}{\rho_0^S}, & \varepsilon &= \frac{\rho_0^F - \rho^F}{\rho_0^F} \end{aligned} \quad (18)$$

The quantity

$$\zeta = n_0 (\varepsilon - e), \quad (19)$$

is called the fluid mass content and it is often used in Biot's model instead of the fluid volume changes, ε . It should be stressed that this variable yields thermodynamical nonequilibrium processes. It becomes zero if the partial velocities are equal: $\mathbf{v}^S = \mathbf{v}^F$, *vis.*

$$\frac{\partial \zeta}{\partial t} = n_0 \frac{\partial}{\partial t} (\varepsilon - e) = \operatorname{div} (\mathbf{v}^F - \mathbf{v}^S), \quad (20)$$

and this corresponds to the lack of diffusion which means thermodynamical equilibrium. This remark has the bearing in variational formulation of field equations for the Biot model. Clearly, such a formulation based on a Lagrangian is not possible if ζ is chosen to be the variable as the equations of motion for such a system are not stationary points of the action functional (e.g. compare [54]).

Summing up, the Biot model of the saturated porous material is described by the following field equations, following from the partial momentum balance equations

$$\begin{aligned}
 \rho_0^S \frac{\partial \mathbf{v}^S}{\partial t} - \rho_{12} \left(\frac{\partial \mathbf{v}^F}{\partial t} - \frac{\partial \mathbf{v}^S}{\partial t} \right) &= \lambda^S \operatorname{grad} e + 2\mu^S \operatorname{div}^S + \\
 &+ Q \operatorname{grad} \varepsilon + \pi * (\mathbf{v}^F - \mathbf{v}^S) + \rho_0^S \mathbf{b}^S, \\
 \rho_0^F \frac{\partial \mathbf{v}^F}{\partial t} + \rho_{12} \left(\frac{\partial \mathbf{v}^F}{\partial t} - \frac{\partial \mathbf{v}^S}{\partial t} \right) &= \rho_0^F \kappa \operatorname{grad} \varepsilon - \\
 &- Q \operatorname{grad} e - \pi * (\mathbf{v}^F - \mathbf{v}^S) + \rho_0^F \mathbf{b}^F,
 \end{aligned} \tag{21}$$

and the kinematic compatibility equations (18)_{1,2}. Obviously, unknown fields are in this model

$$\{\mathbf{v}^S, \mathbf{v}^F, \mathbf{e}^S, \varepsilon\}, \tag{22}$$

while the partial mass densities ρ^S, ρ^F and the porosity n follow from the relations (18)_{3,4} and (17), respectively.

Let us mention that in many works on Biot's model the displacement vectors of both components are used as independent fields. Then

$$\mathbf{v}^S = \frac{\partial \mathbf{u}}{\partial t}, \quad \mathbf{e}^S = \operatorname{sym} \operatorname{grad} \mathbf{u}, \quad \mathbf{v}^F = \frac{\partial \mathbf{U}}{\partial t}, \quad \varepsilon = \operatorname{div} \mathbf{U}, \tag{23}$$

where \mathbf{u} is the displacement vector of the skeleton and \mathbf{U} is the displacement vector of the fluid. The relations (18)_{1,2} are then identities. We shall not use these fields as the displacement field for the fluid is rather artificial for diffusion processes.

For the purpose of further analysis we rewrite the set of equations of the full model (without coupling β and porosity sources \hat{n} !) in Cartesian coordinates

$$\begin{aligned}
 \rho_0^S \frac{\partial v_i^S}{\partial t} - \rho_{12} \left(\frac{\partial v_i^F}{\partial t} - \frac{\partial v_i^S}{\partial t} \right) &= \lambda^S \frac{\partial e}{\partial x_i} + 2\mu^S \frac{\partial e_{ij}^S}{\partial x_j} + \\
 &+ Q \frac{\partial \varepsilon}{\partial x_i} - N \frac{\partial n}{\partial x_i} + \pi * (v_i^F - v_i^S) + \rho_0^S b_i^S, \\
 \rho_0^F \frac{\partial v_i^F}{\partial t} + \rho_{12} \left(\frac{\partial v_i^F}{\partial t} - \frac{\partial v_i^S}{\partial t} \right) &= \rho_0^F \kappa \frac{\partial \varepsilon}{\partial x_i} - \\
 &- Q \frac{\partial e}{\partial x_i} - N \frac{\partial n}{\partial x_i} - \pi * (v_i^F - v_i^S) + \rho_0^F b_i^F,
 \end{aligned} \tag{24}$$

and

$$\frac{\partial e_{ij}^S}{\partial t} = \frac{1}{2} \left(\frac{\partial v_i^S}{\partial x_j} + \frac{\partial v_j^S}{\partial x_i} \right), \quad \frac{\partial \varepsilon}{\partial t} = \frac{\partial v_i^F}{\partial x_i},$$

$$n = n_0 \left(1 + \delta e + \frac{\Phi_0}{n_0} (\varepsilon - e) \right). \quad (25)$$

In the next Section, we investigate the structure of linear relations (10), (11) and some extensions for anisotropic materials.

4. STRUCTURE OF MOMENTUM SOURCE IN THE LINEAR MODEL

Inspection of the set of equations (24), (25) shows that we have to prescribe the following material constants

$$\left\{ K = \lambda^S + \frac{2}{3} \mu^S, \kappa, Q, N, \delta, \Phi_0 \right\}, \mu^S, \rho_{12}, \quad (26)$$

and the hereditary function

$$\pi = \pi(t), \quad (27)$$

in order to make the model applicable for the description of processes in a particular saturated porous material. The set of constants in the curly brackets can be determined by means of the microscopic compressibilities of components, K_s, K_f, K_b (i.e. true compressibilities of the skeleton, of the fluid, and the undrained compressibility modulus, respectively) and the initial porosity, n_0 (see: [85]). There are attempts within “kinetic” models of granular materials to determine the shear modulus μ^S from the analysis of the interactions of granulae. However, in general, it must be assumed that this constant is obtained in some experiments (e.g. by measuring the speed of propagation of transversal waves). The constant ρ_{12} and the parameter π are the subject of discussion of this Section.

We begin with the permeability coefficient π . The classical linear relation in which this parameter appears can be derived from the partial momentum balance equation (4)₃ or (24)₂ if we assume that an influence of inertia is negligible and the coefficient π is a constant. We obtain the following relation

$$\text{grad} p^F + \pi (\mathbf{v}^F - \mathbf{v}^S) - \rho_0^F \mathbf{b}^F = 0, \quad (28)$$

This relation can be written in the form

$$\mathbf{j} = -\frac{\rho_0^F}{\pi} (\text{grad } p^F - \rho_0^F \mathbf{b}^F), \quad \mathbf{j} = \rho_0^F (\mathbf{v}^F - \mathbf{v}^S) \quad (29)$$

where \mathbf{j} is the mass discharge per unit cross-sectional area in the direction of the relative flow $\mathbf{v}^F - \mathbf{v}^S$ [12, 13].

In the original Darcy formulation of the above relation, the mass discharge \mathbf{j} is replaced by the specific volume discharge of the fluid, q [$\text{m}^3/\text{m}^2\text{s}$]. Hence

$$|q| = \frac{1}{\rho_0^F} \mathbf{j} \cdot \frac{(\mathbf{v}^F - \mathbf{v}^S)}{|\mathbf{v}^F - \mathbf{v}^S|} = |\mathbf{v}^F - \mathbf{v}^S|. \quad (30)$$

This quantity describes the volume of the fluid discharge per unit surface perpendicular to the vector $\mathbf{v}^F - \mathbf{v}^S$ and per unit time. In the particular case of a homogeneous material with the z-axis oriented in the direction of the gravitational force, we can integrate (28) and write for the inclined column of a porous medium of the length L :

$$q = k \frac{\varphi_1 - \varphi_2}{L}, \quad \varphi_1 = h_1 + \frac{p_1^F}{\gamma n_0}, \quad \varphi_2 = h_2 + \frac{p_2^F}{\gamma n_0}, \quad (31)$$

$$k = \frac{n_0 \gamma}{\pi}, \quad \gamma = \frac{g \rho_0^F}{n_0},$$

where g is the earth acceleration, $z = h_1$ and $z = h_2$ are the isometric heads at these levels of the column, $(\varphi_1 - \varphi_2)/L$ is called the hydraulic gradient (driving force). The difference $\varphi_1 - \varphi_2$ is called the driving head. The relation (31) is the classical form of Darcy's law and the coefficient k [m/s], is called the hydraulic conductivity. It is sometimes related to the true dynamic viscosity of the fluid in pores [12]

$$k = \frac{\kappa_p \gamma}{\mu_v} \Rightarrow \kappa_p = \frac{n_0 \mu_v}{\pi}, \quad (32)$$

where κ_p , [m^2], is the so-called intrinsic permeability, while μ_v is the true dynamic viscosity of the fluid. We use further the coefficient of permeability π , [$\text{kg}/\text{m}^3\text{s}$] as it appears in the natural way in the momentum source and, consequently, in equations of motion.

In the Table 1 below we show a few examples of hydraulic conductivity, k , intrinsic permeability, κ_p , and permeability coefficient, π , for water in

channels under normal conditions (pressure 10^5 Pa, temperature 20° C, dynamic viscosity $\mu_v = 1.002 \times 10^{-3}$ Pas).

Table 1: Examples of hydraulic conductivity, intrinsic permeability and permeability coefficient for a porous material saturated with water (normal conditions)

soil	k [m/s]	\mathcal{K}_p [darcy]= 10^{-12} [m ²]	π [kg/m ³ s]
well sorted gravel	$1 - 10^{-3}$	$10^5 - 10^2$	$10^3 - 10^6$
oil reservoir	$10^{-4} - 10^{-6}$	$10 - 10^{-1}$	$10^7 - 10^9$
sandstone	$10^{-7} - 10^{-8}$	$10^{-2} - 10^{-3}$	$10^{10} - 10^{11}$
granite	$10^{-11} - 10^{-12}$	$10^{-6} - 10^{-7}$	$10^{14} - 10^{15}$

A constant scalar quantity describing the permeability is in various applications not sufficient to describe the diffusion in porous media. Three important generalizations are particularly important. The first one is related to different properties of channels in different directions. This yields the anisotropy and the dependence on the curvature of channels, i.e. on the tortuosity. The second one is related with nonlinear effects. This may be, for instance, a nonlinear dependence of the momentum source on the relative velocity. It may appear in the case of flows with a high Reynolds number. In porous materials, for values higher than app. 10 (for pipes this value is much higher and may even reach 2000), there is an essential influence of the curvature of channels (tortuosity) and for values higher than 100 the flow becomes turbulent [44] and many structural effects such as liquefaction may appear [12, 81]. P. Forchheimer [36] (see [64] for details) has introduced the simplest extension of Darcy's relation by an additional contribution quadratic in relative velocity. This relation is still frequently used for turbulent flows in porous materials. The third generalization follows from viscous properties of fluids in channels. It has been investigated by M. A. Biot [19] who has shown that, for monochromatic waves, the coefficient π must be frequency-dependent for high frequencies (see Section 6). This yields a time-dependence (hereditary effect) of this coefficient in a general case and, consequently, the convolution integral in the momentum source. We shall not discuss any nonlinear effects in this paper. However, we return further to the problem of frequency dependence. In this Section we discuss anisotropy and tortuosity effects.

Anisotropy of the diffusion is a consequence of the complex microstructure of porous materials. In particular, geometry of channels induces complicated shapes of true streamlines while, on the macroscopic level, the average flow may be even one-dimensional. This has been recognized early in the description of diffusivity. J. Kozeny [47] proposed the proportionality of the inverse of hydraulic conductivity k to the so-called tortuosity, τ . It was defined as the ratio of the true length, L_e , of the streamline between two points to the

distance between these two points, L , i.e. $\tau = L_e / L$ (e.g. [61]) Obviously, this quantity is not smaller than unity, $\tau \geq 1$. Consequently, in local terms, its inverse is the average value of the cosine of the angle between the tangent to the macroscopic (average) streamline and the tangent to the true streamline. This relation, the so-called Blake-Kozeny equation, has been later on corrected as the dependence on the tortuosity should be quadratic (see: [30, 34]). In our notation it has the following form [34]

$$K = \frac{k}{\gamma n_0} = \frac{D_h^2 n_0}{b \mu_v \tau^2}, \quad (33)$$

where b is the so-called capillary shape factor (e.g. 32 for circular pores and 48 for parallel slits) and D_h denotes the hydraulic diameter.

For a packed bed of spheres of uniform diameter d , the representative elementary volume *REV* (i.e. the domain of microstructure which is macroscopically identified with a single material point) contains N such spheres. Consequently, the volume occupied by the fluid and the wetted surface in such a volume are

$$\begin{aligned} V_f &= \frac{1}{6} \pi d^3 N \frac{n_0}{1-n_0}, \quad S_s = \pi d^2 N \Rightarrow \\ \Rightarrow D_h &= 4 \frac{V_f}{S_s} = \frac{2}{3} d \frac{n_0}{1-n_0}. \end{aligned} \quad (34)$$

Then the hydraulic conductivity K has the form

$$K = \frac{4d^2}{9b\mu_v\tau^2} \frac{n_0^3}{(1-n_0)^2} \Rightarrow \pi = \frac{9}{4} \frac{b\mu_v}{d^2} \tau^2 \left(\frac{1-n_0}{n_0} \right)^2, \quad (35)$$

where the coefficient $9b\tau^2/4$ is often assumed to be equal 180. For $b = 33.3$ it corresponds to the tortuosity $\tau = 1.56 \approx \pi/2$. In the next Section we return to experimental values of this quantity.

It is clear that values of tortuosity τ may depend on the direction of the flow through the porous medium. Josef Kubik [48, 50] was most likely the first who investigated such a model. A systematic derivation of macroscopic description of anisotropic diffusion based on the averaging procedures for microstructures of porous materials was done by Jacob Bear and Yehuda Bachmat [12, 7, 13, 14, 15]. In the book [7] they present the derivation of transformation rules for various quantities of microscopic equations of motion under the action of the volume averaging procedure over the Representative

Elementary Volume (*REV*). One of the fundamental results are the rules for the pressure gradient and for the interstitial velocity which yield a modification of Darcy's law. For instance, the averaging procedure for a gradient of any quantity on the level of microstructure yields two contributions. The first one is the macroscopic gradient of the average of this quantity transformed by a matrix, T_{ij} , related to the structure of channels and called the tortuosity tensor while the second one is a surface average of the microstructural gradient (see formula (2.348) in [13]). If we leave out various correlation terms, we arrive at the following generalization of Darcy's formula

$$q_i = -\frac{k_{ij}}{n_0 \gamma} \left(\frac{\partial p^F}{\partial x_j} + \rho^F g \frac{\partial z}{\partial x_j} \right), \quad (36)$$

where $\mathbf{q} = q_i \mathbf{e}_i$ is the vector of the specific discharge and it is assumed that the z -axis is chosen in the direction of the earth acceleration. The symmetric permeability tensor k_{ij} possesses the following structure

$$k_{ij} = B T_{ij}, \quad (37)$$

where the symmetric tortuosity tensor, T_{ij} , is defined as the following surface average (the static moment of the *REV* boundary intersected by streamlines with respect to a chosen center of *REV*) [13]

$$\mathbf{T} = T_{ij} \mathbf{e}_i \otimes \mathbf{e}_j = \frac{1}{n_0 V} \int_{S_s(\mathbf{r})} \mathbf{n} \otimes \mathbf{r}' dS, \quad V = \text{volume}(\text{REV}), \quad (38)$$

where S_s is the part of the boundary of the representative elementary volume, ∂REV , intersecting pores, \mathbf{n} is the unit normal to this surface and, simultaneously, tangent to the streamline intersecting S_s at the point \mathbf{r}' . The unit base vectors \mathbf{e}_i are chosen to be the same for macroscopic and microscopic local coordinates

$$\mathbf{r} = x_i \mathbf{e}_i, \quad \mathbf{r}' = \xi_i \mathbf{e}_i, \quad \mathbf{r} = x_i \mathbf{e}_i, \quad \mathbf{r}' = \xi_i \mathbf{e}_i, \quad (39)$$

while the unit vector \mathbf{n} tangent to the streamline is given by the standard relation

$$\mathbf{r}' = \mathbf{r}'(s), \quad \mathbf{n} = \frac{d\xi_i}{ds} \mathbf{e}_i, \quad (40)$$

where s is the parameter along the streamline.

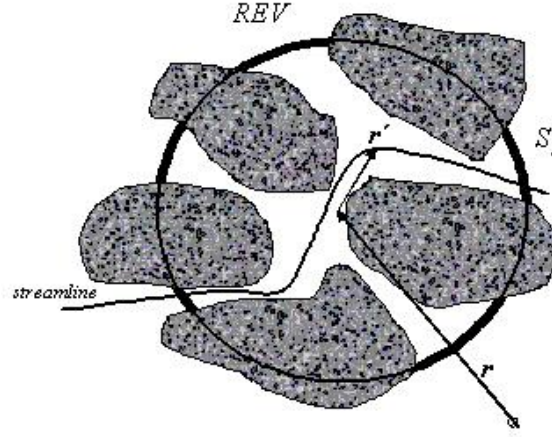


Fig. 7. Schematic of the Representative Elementary Volume with a streamline intersecting the REV -boundary at a point of the surface S_s . The latter is indicated by the thick line. \mathbf{r} is the position vector of the REV -center and \mathbf{r}' is the local position vector within REV

If we choose REV to be a sphere of radius R then the definition (38) has the form

$$\mathbf{T} = T_{ij} \mathbf{e}_i \otimes \mathbf{e}_j = \frac{1}{n_0 V} \int_{S_s} R \mathbf{n} \otimes \mathbf{n} dS \quad (41)$$

which demonstrate the symmetry of the tortuosity tensor. If we solve the eigenvalue problem for this tensor then

$$\mathbf{T} = \sum_{\alpha=1}^3 T^{(\alpha)} \mathbf{t}^{(\alpha)} \otimes \mathbf{t}^{(\alpha)}, \quad (42)$$

where $T^{(\alpha)}$ are eigenvalues of the tortuosity tensor and $\mathbf{t}^{(\alpha)}$ its eigenvectors. It is easy to see from the definition (41) that the eigenvalues are positive and smaller than one. In the case of isotropic microstructure (random distribution of grains or curvy channels) we have

$$T^{(1)} = T^{(2)} = T^{(3)} = \frac{1}{\tau^2} \quad (43)$$

The last relation was proved by J. Bear [12].

In the isotropic case, we can immediately identify the conductance B of the relation (37). For instance, in terms of the hydraulic diameter D_h ,

$$B = \frac{D_h^2 \gamma n_0^2}{b \mu_v} \quad \text{or} \quad B = \kappa_p \frac{\gamma}{\mu_v} \tau^2. \quad (44)$$

For the coefficient of permeability, we obtain

$$\pi = \pi_0 \tau^2, \quad \pi_0 = \frac{n_0 \gamma}{B}. \quad (45)$$

Hence, as expected, the higher values of viscosity μ_v and of the tortuosity τ yield higher values of dissipation (15). On the other hand, the bigger values of conductance B (due to, for instance, bigger hydraulic diameter D_h or bigger porosity n_0) yield smaller dissipation.

For anisotropic materials without hereditary properties one can write now a generalization of the constitutive law (13) for the momentum source. Bearing the relations (13), (37) and (45) in mind we have

$$\hat{p}_i^S = \pi_0 T_{ij}^{-1} (v_j^F - v_j^S) - \rho_{12} a_{ri}, \quad \mathbf{a}_r = a_{ri} \mathbf{e}_i, \quad (46)$$

where T_{ij}^{-1} is the inverse of the tortuosity tensor. In principal base vectors (eigenvectors) it has the following spectral representation

$$\mathbf{T}^{-1} = T_{ij}^{-1} \mathbf{e}_i \otimes \mathbf{e}_j = \sum_{\alpha=1}^3 \frac{1}{T^{(\alpha)}} \mathbf{t}^{(\alpha)} \otimes \mathbf{t}^{(\alpha)}. \quad (47)$$

It should be stressed that the above considerations concerning anisotropic properties of diffusion are based on many simplifying assumptions concerning laminar flows, and, consequently, linearity with respect to the relative velocity of components, small deformations of the skeleton and of the fluid, very simple statistical properties of the microstructure, etc. More sophisticated models are missing as yet. In Section 6, we return to a correction of this model by introducing hereditary properties.

We proceed to a few remarks on the added mass effect, described by the coefficient ρ_{12} . The problem of added mass was discovered in relation to the so-called d'Alembert paradox: for incompressible and inviscid potential flow the drag force on a body moving with constant velocity is zero in the infinite medium. It has been shown (e.g. §11 in [52]) that the fluid is acting on the body with a force which creates the inertial force proportional to a mass bigger than the mass of the body. D'Alembert paradox has been explained within the mechanics of viscous fluids. This has been the motivation for M. A. Biot to introduce the coupling through the added mass. If we write the equation (21)₂ for the one-dimensional case in the following form

$$\rho_{12} \frac{\partial v_x^S}{\partial t} + Q_x^F = 0, \quad Q_x^F = \rho_0^F \kappa \frac{\partial \varepsilon}{\partial x} - Q \frac{\partial e}{\partial x} - \pi * (v_x^F - v_x^S) + \rho_0^F b_x^F, \quad (48)$$

then the argument of M. A. Biot [18] is as follows: “...the equation shows that when the solid is accelerated a force Q_x^F must be exerted on the fluid to prevent an average displacement of the latter”. This is obviously not necessary. First of all, Biot did not have a contribution of relative velocity in his work [18] – it has been introduced in his later works. This contribution results, as we have already described, from the viscosity of the fluid (see also a remark of J. Bear, p.104 in [12]). Consequently, d’Alembert paradox does not appear in these models. Secondly, the lack of an inertial term in (48) does not mean that a motion of the skeleton does not influence the “displacement” of the fluid, as the structure of the force Q_x^F clearly shows. In addition, the paradox appears only in cases of ideal fluids in infinite domains without a boundary which is, of course, not the case in porous materials.

However, the above argument does not mean that the added mass cannot appear in the model. As indicated by Coussy (p. 40 in [31]) and Bourbie, Coussy, Zinszner (p. 71 in [25]) it may be related to fluctuations of the interstitial velocity. In the books [25, 31] the Authors refer to ρ_{12} as related to the tortuosity. This relation seems to be wrong as tortuosity always yields dissipation and the added mass effect is nondissipative. As we have pointed out in Section 3 (formula (14)) the added mass yields nonlinear stress reactions of components. Similarly to ρ_{12} , this can hardly be measured. We return to this issue in the Section 6 on waves.

5. NMR PRIMER. DIFFUSION MRI METHODS FOR DETERMINATION OF DIFFUSION PARAMETERS; SOME RESULTS OF GEOPHYSICAL EXPERIMENTS

Experimental assignment of material parameters to a model of porous materials relies on two types of procedures. Either randomly extracted samples are investigated in a laboratory and then the experiment is invasive or the material is checked *in situ* which means that the experiment is nondestructive. Particularly, in medical applications and in experiments on granular materials the second type of the procedure is preferable. Two such methods are commonly used. The first one uses the properties of mechanical waves, in particular, their speeds of propagation, attenuation und scattering. We return to these acoustical methods in the next Section. The second type relies on magnetic properties of materials. It is

particularly useful in investigation of diffusion. In this Section, we present some basic features and results of this NMR method.

Nuclear magnetic resonance (NMR) is a property possessed by nuclei in a magnetic field and applied electromagnetic pulses. Quantum mechanical subatomic particles, i.e. protons, neutrons and electrons possess the spin. In some atoms like ^{12}C , ^{16}O , ^{32}S , these spins cancel out each other and the nucleus has the zero spin. In many other atoms such as ^1H , ^{13}C , ^{31}P , ^{15}N , ^{19}F , the nucleus possesses a nonzero spin. In order to determine the overall spin one can use the following rules (e.g. [32]): (1) If the number of neutrons and the number of protons are both even then the nucleus has no spin. (2) If the number of neutrons plus the number of protons is odd then the nucleus has a half-integer spin, i.e. $1/2$, $3/2$, $5/2$. (3) If the number of neutrons and the number of protons are both odd, then the nucleus has an integer spin i.e. 1, 2, 3.

Based on this observation quantum mechanics yields a theoretical description of interactions of spin nuclei with external magnetic fields which forms the foundation of NMR testing methods. We present here only a few remarks on this subject following the presentation of Ch. Epstein [33] and B. Blümich [22].

We begin with a model of a proton. The proton is a spin-1/2 particle. The spin state of the proton is described by the wave function ψ . The intrinsic magnetic moment of proton, $\boldsymbol{\mu}_p$, and its intrinsic angular momentum, \mathbf{J}_p , are quantum mechanical observables. They are related to each other in the following manner

$$\boldsymbol{\mu}_p = \gamma_p \mathbf{J}_p, \quad (49)$$

where γ_p is the gyromagnetic ratio. For hydrogen protons in water molecules

$$\gamma_p = 2\pi \times 42.5764 \times 10^6 \frac{\text{rad}}{\text{Tesla}}. \quad (50)$$

The time evolution of the wave function ψ is described by Schrödinger equation

$$\hbar \frac{\partial \psi}{\partial t} = i \mathbf{B} \cdot \boldsymbol{\mu}_p \psi, \quad (51)$$

where $\hbar = 1.0545 \times 10^{-27}$ ergsec denotes Plank's constant and

$$\mathbf{B} \cdot \boldsymbol{\mu}_P = \frac{\gamma_P \hbar}{2} [B_x \sigma_x + B_y \sigma_y + B_z \sigma_z]$$

$$\sigma_x = \begin{pmatrix} 0 & 1 \\ 1 & 0 \end{pmatrix}, \quad \sigma_y = \begin{pmatrix} 0 & -i \\ i & 0 \end{pmatrix}, \quad \sigma_z = \begin{pmatrix} 1 & 0 \\ 0 & -1 \end{pmatrix}, \quad (52)$$

the σ -matrices are called Pauli spin matrices.

The macroscopic behaviour of these quantities is described through the so-called expectations of observables of a quantum mechanical model. For the intrinsic magnetic moment and the intrinsic magnetic momentum they have the form of inner products

$$\langle \mathbf{J}_P \rangle = \langle \mathbf{J}_P \psi, \psi \rangle,$$

$$\langle \boldsymbol{\mu}_P \rangle = \langle \boldsymbol{\mu}_P \psi, \psi \rangle. \quad (53)$$

Then Schrödinger equation implies the following equation for the expectation of $\boldsymbol{\mu}_P$

$$\frac{d\langle \boldsymbol{\mu}_P \rangle}{dt} = \gamma_P \langle \boldsymbol{\mu}_P \rangle \times \mathbf{B}. \quad (54)$$

The solution of this equation for a static magnetic field $\mathbf{B} = \mathbf{B}_0 = b_0 \mathbf{e}_3$ is particularly instructive. Equations (54) have in this case the following form for the components $\langle \boldsymbol{\mu}_P \rangle = \langle \mu_P \rangle_i \mathbf{e}_i$

$$\frac{d\langle \mu_P \rangle_1}{dt} = \gamma_P b_0 \langle \mu_P \rangle_2, \quad \frac{d\langle \mu_P \rangle_2}{dt} = -\gamma_P b_0 \langle \mu_P \rangle_1, \quad (55)$$

and $\langle \mu_P \rangle_3$ is a constant. Hence

$$\frac{d^2\langle \mu_P \rangle_1}{dt^2} + \gamma_P^2 b_0^2 \langle \mu_P \rangle_1 = 0,$$

$$\frac{d^2\langle \mu_P \rangle_2}{dt^2} + \gamma_P^2 b_0^2 \langle \mu_P \rangle_2 = 0, \quad (56)$$

Consequently, the solution for these two components is proportional to $\exp(-\omega_0 t)$, $\omega_0 = \gamma_P b_0$. This type of motion is called the precession. The frequency ω_0 is called the Larmor frequency. These properties indicate that the proton reacts on the action of an external magnetic field

$\mathbf{B}_1 = b_1 \cos \omega t \mathbf{e}_1 + b_1 \sin \omega t \mathbf{e}_2$ and for equal frequencies: $\omega = \omega_0$ there appears the resonance. This can be observed experimentally as the sudden growth of the amplitude of the field. It is important to notice that the resonance Larmor frequency is in the order of 100 MHz for external b_0 -fields of the order of 1 Tesla (compare (50)). For comparison, the magnetic field of earth is app. 5×10^{-5} Tesla.

Spin nuclei in substances such as water interact with each other. Hence, the simple equation (54) does not hold anymore and we have to construct a macroscopic model. If $\rho(\mathbf{r})$ denotes the density of a substance, say water, which carries the spin nuclei then, placed in a static magnetic field $\mathbf{B}_0(\mathbf{r})$ the spins become polarized and produce a net bulk magnetization $\mathbf{M}_0(\mathbf{r})$. The strength of this field is determined by a macroscopic thermodynamic relation

$$\mathbf{M}_0(\mathbf{r}) = \frac{C}{T} \rho(\mathbf{r}) \mathbf{B}_0(\mathbf{r}), \quad (57)$$

where T is the absolute temperature. Felix Bloch [21] introduced a phenomenological equation describing the bulk magnetization resulting from the interaction of nuclear spins with each other and with an external field. For an external field

$$\mathbf{B}(\mathbf{r}, t) = \mathbf{B}_0(\mathbf{r}) + \tilde{\mathbf{B}}(\mathbf{r}, t), \quad (58)$$

where the time dependent part $\tilde{\mathbf{B}}(\mathbf{r}, t)$ is much smaller than the static part, the magnetization $\mathbf{M}(\mathbf{r}, t)$ is assumed to satisfy the following Bloch equation

$$\begin{aligned} \frac{d\mathbf{M}}{dt} &= \gamma \mathbf{M} \times \mathbf{B} - \frac{1}{T_2} \mathbf{M}^\perp - \frac{1}{T_1} (\mathbf{M}^\parallel - \mathbf{M}_0), \\ \mathbf{M} &= \mathbf{M}^\perp + \mathbf{M}^\parallel, \end{aligned} \quad (59)$$

with \mathbf{M}^\parallel (longitudinal part) parallel to \mathbf{B}_0 and \mathbf{M}^\perp (transversal part) perpendicular to \mathbf{B}_0 . T_1 and T_2 are longitudinal relaxation time (recovery time) and transverse relaxation time, respectively.

The gyromagnetic constant appearing in (59) and determining the resonance frequency is a material parameter. Some examples of its values for various atoms are shown in Table 2. It is clear that for the same external magnetic field $\mathbf{B}_0 = b_0 \mathbf{e}_3$ the resonance frequency ω_0 will be different for

different substances. For examples listed in Table 2 it varies between app. 19 and 270 MHz for the external field of 1 Tesla.

Table 2: Some values of the gyromagnetic constant γ

Nucleus	^1H	^2H	^3He	^7Li	^{13}C	^{14}N
γ ($10^6 \text{ rad.s}^{-1}.\text{T}^{-1}$)	267.513	41.065	203.789	103.962	67.262	19.331

Nucleus	^{15}N	^{17}O	^{23}Na	^{31}P	^{129}Xe
γ ($10^6 \text{ rad.s}^{-1}.\text{T}^{-1}$)	27.116	36.264	70.761	108.291	73.997

The equation (59) can be solved for various external (secondary) fields $\bar{\mathbf{B}}$. These secondary fields are called RF-fields – Radio Frequency fields – due to the range of their frequency yielding the resonance. In basic measurements the sample is polarized by the constant field \mathbf{B}_0 and then an RF-excitation is turned on for a finite time t_{exc} . After that time the RF is turned off. The vector field $\mathbf{M}(\mathbf{r}, t)$ precesses about \mathbf{B}_0 in phase with the angular velocity ω_0 . The corresponding solution of (59) has the form

$$\mathbf{M}(\mathbf{r}, t) = \frac{C\omega_0\rho(\mathbf{r})}{\gamma T} \left[e^{-t/T_2} \cos(\omega_0 t + \phi) \mathbf{e}_1 + e^{-t/T_2} \sin(\omega_0 t + \phi) \mathbf{e}_2 + \left(1 - e^{-t/T_1}\right) \mathbf{e}_3 \right] \quad (60)$$

where ϕ is a constant phase. Hence, the transverse components $M_x \mathbf{e}_1$ and $M_y \mathbf{e}_2$ decay exponentially with the transverse relaxation time T_2 . The component $M_z \mathbf{e}_3$ reduces after the relaxation with the longitudinal relaxation time T_1 to the form (57). Further analytical details can be found in the work of Ch. Epstein [33].

Both relaxation times follow from combinations of various relaxation processes. For instance, the transverse relaxation time is a weighted average of the surface-liquid relaxation time and the relaxation time of the bulk liquid [5]. This gives rise to NMR methods of investigation of the area of wetted surfaces, degrees of saturation etc. As the model discussed in this paper is two-component we cannot describe the saturation problems. Hence, wetting problems (capillary-bound water), degree of saturation etc. are not presented in this work. However, it should be mentioned that NMR measurements deliver data on these quantities [69, 70].

In practical applications to NMR imaging a multipulse excitation by a gradient magnetic field is applied and the orientation of the z-axis is changed. In this way one can obtain tomographic three-dimensional pictures of the system (the principles of this testing are explained, for instance in B. Blümich [22], p. 54).

Measurements of relaxation times yield estimates of parameters of porous materials through certain calibration procedures which we shall not present in this work (e.g. see [6])². For instance, transverse relaxation time measurements lead directly to the estimation of porosity. Traditionally in geophysics, the total porosity is subdivided into three major components: free-fluid porosity with long T_2 ($T_2 > 33$ ms), capillary-bound water ($3 > T_2 > 33$ ms) and clay-bound water ($T_2 < 3$ ms). Porosity is determined by the normalization of the signal amplitude measured on water-saturated samples by the amplitude measured on pure water. Obviously, the latter corresponds to 100% porosity.

It should also be mentioned that it is rather recent to apply gas phase NMR in nondestructive testing as the mass density of the gas was long considered to be too small. The advent of the spin-exchange optical pumping technique for noble gases allows to use NMR methods, for instance, in investigation of lung space and many other porous media [56].

The instrumentation for the NMR nondestructive testing develops very rapidly. These are not only robust NMR tomographs for medical diagnosis but also many field devices for applications in geophysics (e.g. Halbach core-scanner [6] or NMR-mouse [22]).

Results of NMR measurements, as all results obtained by ill-posed inverse methods, yield nonuniqueness which must be eliminated by some additional measurements. In geophysics these are often geoelectric measurements (for theoretical foundations, see [58]) or radar measurement [90, 91].

The Bloch model has been extended after an observation of E. Hahn [41] in 1950 that the diffusion influences the nuclear magnetic resonance. In 1956 H.

² Diffusion magnetic resonance methods have been discovered in 1990 by Michael Moseley who pointed out that the water diffusion in white matter is anisotropic. Since then the magnetic resonance imaging became one of the most important tests in medicine. We quote here only a few representative papers on this subject [6, 9, 10, 11, 16, 42, 55, 57]. It is also indicated that the tortuosity is coupled not only to geometrical properties of the system but to the viscosity of the fluid as well [67]. This may have an important consequences in medical diagnosis procedures.

On the other hand, diffusion magnetic resonance method in geophysics is used rather to measurements of various microstructural parameters. Most important are the porosity and tortuosity. The method is used in testing rocks [82379] but it becomes important also in experiments on sands [24, 62].

C. Torrey [75] proposed the following extension, the so-called Bloch - Torrey equation

$$\frac{d\mathbf{M}}{dt} = \gamma \mathbf{M} \times \mathbf{B} - \frac{1}{T_2} \mathbf{M}^\perp - \frac{1}{T_1} (\mathbf{M}^\parallel - \mathbf{M}_0) + \text{div}(\mathbf{D} \text{grad} \mathbf{M}),$$

$$\mathbf{D} = D_{ij} \mathbf{e}_i \otimes \mathbf{e}_j, \quad (61)$$

where \mathbf{D} is the diffusion tensor. Clearly, this extension yields the possibility of the description of anisotropic tortuosity which we have presented earlier. Equation (61) yields a modification of the classical MRI (magnetic resonance imaging) method called DWI – diffusion weighted MRI. Up to now it is intensively developed in medical applications. A typical result of the application of this method is shown in Fig. 8.

In Tables 3 and 4 we present some examples of experimental results obtained by methods of the nuclear magnetic resonance. Table 3 contains data for some rocks on which the measurements were performed with the help of the noble gas Xenon filling the pores.

Table 3: Results of Xenon NMR measurements for some rocks [77]

Rock Sample	Permeability \mathcal{K}_p [mD]; π [kg/m ³ s]	Tortuosity	Effective Porosity	Absolute Porosity (pycnometer)
Fontainebleau	559 ± 93 ; $1.53-2.15 \times 10^8$	3.45	0.113 ± 0.007	0.125
Bentheimer	123 ± 24 ; $10.1-6.8 \times 10^8$	NA	0.112 ± 0.012	NA
Edwards Limestone	7.0 ± 0.9 ; $1.27-1.63 \times 10^{10}$	4.76	0.151 ± 0.011	0.233
Austin Chalk	2.6 ± 0.3 ; $3.44-4.35 \times 10^{10}$	5.58	0.184 ± 0.9	0.297
Cutbank H	0.64 ± 0.1 ; $1.35-1.65 \times 10^{11}$	NA	0.0603 ± 0.004	NA
Indiana Limestone	0.18 ± 0.03 ; $4.76-6.67 \times 10^{11}$	7.69	0.071 ± 0.006	NA

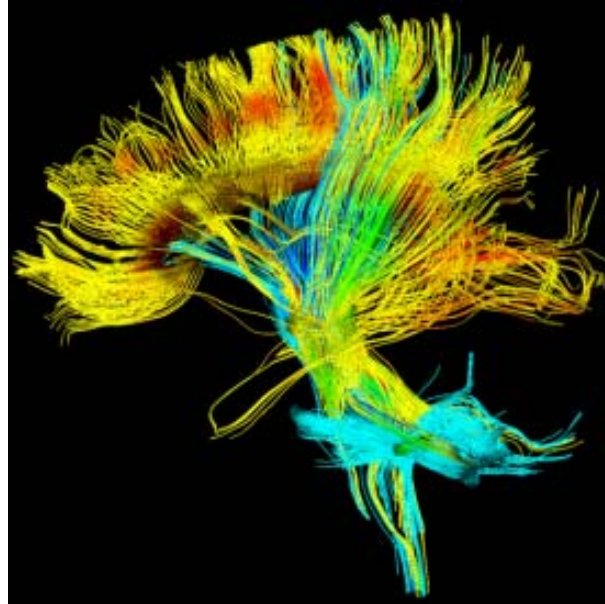


Fig. 8. An example of diffusion MRI: tractography of major brain white matter tracts computed from the local diffusion tensor eigenvectors (syngo.via, Siemens)

Table 4: Some results for core plugs of Alermoehe sandstone from various depths [6]

Sample	Permeability (gas):+ K_p [mD]; π [kg/m ³ s]	Tortuosity	Porosity (pycnometer)
3224.45 [m]	0.16; 6.25×10^{11}	1.06	0.02
3235.34 [m]	11.6; 8.62×10^9	5.04	0.09
3236.79 [m]	3.59; 2.79×10^{10}	5.36	0.08
3240.69 [m]	20.7; 4.83×10^9	3.8	0.11
3241.44 [m]	3.13; 3.19×10^{10}	6.12	0.09

Table 4 contains results quoted after [6] for the same rock – sandstone but for samples extracted at the different depth. These results are shown to illustrate the scattering of values of porosity and tortuosity for similar morphologies.

6. PROPAGATION OF BULK ACOUSTIC WAVES IN SATURATED MATERIALS

We proceed now to the investigation of some properties of acoustic waves in two-component poroelastic materials described by equations (24), (25). We limit the attention to isotropic materials but we account for the hereditary properties which have been mentioned in Section 3. This problem is placed in Section on waves as the time dependence of the permeability has been first considered by M. A. Biot [19] for monochromatic waves.

In order to find the time dependence of the permeability coefficient M. A. Biot considered two problems of viscous flow through channels: (1) between parallel walls and (2) in a circular duct in which all quantities are time-dependent in a harmonic way through the factor $e^{i\omega t}$ (Biot denotes the frequency ω by α). Certainly, this may be considered as a Fourier transform of the problem. For those solutions he calculated an average velocity through a cross-section (discharge velocity) and the frictional stresses on the walls. The fraction of these two quantities – a resistance coefficient to the flow - defines a dimensionless function $F(\omega)$ which is supposed to describe frequency dependence of the permeability. For the two cases of the flow Biot obtained the following results

$$(1) \quad F(\omega) = \frac{1}{3} \frac{\sqrt{i\xi} \tanh(\sqrt{i\xi})}{1 - \frac{1}{\xi\sqrt{i}} \tanh(\sqrt{i\xi})}, \quad \xi = a \sqrt{\frac{\omega\mu_v}{\rho}}, \quad (62)$$

$$(2) \quad F(\omega) = \frac{1}{4} \frac{\xi T(\xi)}{1 - \frac{2}{i\xi} T(\xi)}, \quad T(\xi) = \frac{d}{d\xi} \left(\frac{J_0(i\sqrt{i\xi})}{J_0(i\sqrt{i\xi})} \right),$$

where $2a$ is the distance of the walls in the first case and the diameter of the duct in the second case. μ_v, ρ denote the viscosity and the mass density of an incompressible fluid in the channels. J_0 is the Bessel function.. Biot demonstrated the behaviour of the real and imaginary parts of these two functions and found out that their properties are for both cases very similar (see: Fig. 9). This indicates that for an arbitrary shape of the cross-section of the

channel one can use one of those functions with an appropriate choice of the diameter a .

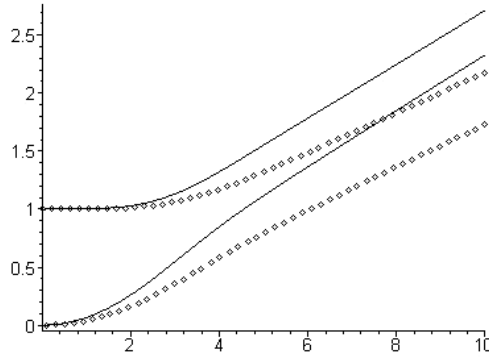


Fig. 9. Real (upper curves) and imaginary (lower curves) parts of functions $F(\xi)$ where ξ is given by (62). Solid lines correspond to the case of parallel walls and dotted lines to the circular duct

In the next step these functions were introduced in the macroscopic equations of motion of components. The x-component of the momentum source is written by Biot in the following bogus form (eqn. (4.2) in [19])

$$\hat{p}_x^S = bF(\omega) \frac{\partial}{\partial t} (U_x - u_x), \quad (63)$$

where b is a constant and U_x, u_x are time dependent x-components of the displacement of the fluid and of the skeleton, respectively. This is, obviously, a combination of the Fourier transformed function $F(\omega)$ with the time dependent velocities. Properly, one should multiply in (63) the transform $F(\omega)$ with the Fourier transform of the relative velocity and the result would be the Fourier transform of the momentum source. One could, of course, inverse as well the transform $F(\omega)$

$$F(t) = \frac{1}{2\pi} \int_{-\infty}^{\infty} F(\omega) e^{i\omega t} d\omega, \quad (64)$$

and then the relation (63) would have the form of the convolution (faltung) integral (11). In contrast to $F(\omega)$ the function $F(t)$ would be real. For isotropic materials one would have then

$$\pi(t) = \pi_0 \tau^2 F(t), \quad (65)$$

where π_0 is given by (44), (45) and τ denotes the tortuosity. The above mistake has been repeated in numerous works on acoustics of porous media (e.g. [25, 46]).

M. A. Biot argued as well that the frequency dependence of the permeability can be neglected for low frequencies ($\lim_{\omega \rightarrow 0} F(\omega) = 1$). For geophysical applications such an assumption is justified as relevant monochromatic wave frequencies lie below a few kilohertz. We consider such an approximation in examples which we present further in this Section.

However, one should mention that the range in which the real part of $F(\omega)$ is essentially different from unity and the imaginary part essentially different from zero lie for values of ξ bigger than app. one, i.e., according to the relation (62), app. 10^{12} 1/s for water in normal conditions and the average diameter of channels app. 1 mm. For smaller diameters this frequency is, of course, higher. This indicates that the high-frequency correction by the function $F(\omega)$ does not have to be made for usual frequency ranges between 1 Hz up to 3 MHz. The last frequency is a maximum frequency admissible for biological tissues. Higher frequencies yield local heating and destruction of biological cells.

Now we return to the issue of the constant ρ_{12} presented already at the end of Section 4. In the poroacoustics this parameter is often considered, similarly to the permeability, to be a function of frequency of monochromatic waves. This has been proposed in 1987 by D. L. Johnson *at al.* [46]. In this paper the flow of the fluid with the mass density ρ_f ($=\rho^{FR}$, i.e. $\phi\rho_f = \rho^F$ in the notation of the present paper), the (macroscopic) velocity \mathbf{v} ($=\mathbf{v}^F$ in the notation of the present paper) is considered to be caused by the (macroscopic) pressure gradient $-\nabla P e^{i\omega t}$. Then the following argument is made:

“Under the stated assumptions \mathbf{v} is obviously linearly related to the pressure gradient at any frequency

$$\tilde{\alpha}(\omega)\rho_f \frac{\partial \mathbf{v}}{\partial \mathbf{t}} = -\nabla P, \quad \phi \mathbf{v} = -\frac{\tilde{k}(\omega)}{\eta} \nabla P. \quad (2.1a,b), \quad (66)$$

($\eta = \mu_v$ in the notation of the present paper). The frequency-dependent tortuosity $\tilde{\alpha}(\omega)$ is defined in (2.1a) by analogy with the response of an ideal

(nonviscous) fluid. ... The frequency –dependent permeability $\tilde{k}(\omega)$ is defined in (2.1b) by analogy with the steady-state ($\omega = 0$) definition.”

Apart from the fallacy of the notation in (66) which we have already discussed earlier the argument made in the comparison of the above relations is wrong from the physical and from the mathematical point of view. Physically, both equations (66) follow as special cases from the same momentum balance equation. The first one follows if the diffusive force in the porous medium is negligible but the inertia is not and the second one follows when the inertia is negligible and the diffusion force is not. It is obvious that one cannot made conclusions on material parameters by comparing these two special limit cases. It is an example of comparing apples and oranges. Mathematically, the first equation yields a hyperbolic (wave) problem and the second one the parabolic (diffusion) problem. Solutions of these two problems belong to two different classes and cannot lead to any *a posteriori* conclusions on material parameters of both models.

Consequently, the relation (4.1b) of the paper [46]

$$" \tilde{\rho}_{12}(\omega) = -[\tilde{\alpha}(\omega) - 1] \phi \rho_f \quad (4.1b) " \quad (67)$$

($\phi = n_0$ in the notation of the present paper) is wrong as well. A common claim that $\tilde{\rho}_{12}$ is measurable is based on this relation and on electrical conductivity measurements of $\tilde{k}(\omega)$ by the use of Archie’s formula. Hence, also this statement is wrong.

We proceed to the presentation of some properties of monochromatic waves in two-component porous materials. There is a very extensive literature of this subject (e.g. [2, 3, 4, 25, 49, 51, 68, 72, 80, 84, 87, 88]). Most of these papers and books contain a spectral analysis of bulk and surface waves. These problems can be considered to be a far-field approximation of the wave problem. Not much has been done on sources of waves and near-field approximations in porous materials. However, this far-field analysis is sufficient for the formation of nondestructive acoustic methods of testing porous materials. For this reason, we limit the attention in this work also to such an analysis of plane monochromatic waves.

We shall use equations (24), (25) with the simplifying assumptions that $\rho_{12} = 0$ (no added mass effect), $N = 0$ (no coupling through the porosity gradient). The former assumption is justified by a numerical analysis which yields the conclusion that Berryman’s relation (67) yields an unacceptable result [87]. Namely, the growing “tortuosity” $\tilde{\alpha}$ yields according to this relation a rapidly decaying attenuation of waves (Fig. 4 in [87]). This is, of course, unacceptable as the tortuosity must increase the dissipation and, consequently,

attenuation of waves. The latter assumption is not very restrictive as in the linear model this coupling can be included in the coupling through volume changes by an appropriate adjustment of the coupling constant Q (see: [85] for details). Changes of porosity described by the second equation (25) do not influence the behaviour of waves because the current porosity does not enter momentum balance equations in the linear model. We investigate the following monochromatic plane wave problem

$$\begin{aligned} v_i^S &= V_i^S \mathcal{E}, & v_i^F &= V_i^F \mathcal{E}, & e_{ij}^S &= E_{ij}^S \mathcal{E}, & \varepsilon &= E^F \mathcal{E}, \\ \mathcal{E} &= \exp[i(k_j x_j - \omega t)] \end{aligned} \quad (68)$$

The amplitudes $V_i^S, V_i^F, E_{ij}^S, E^F$ are assumed to be constant and the wave vector $k_i = kn_i$, $n_i = k_i/k$, $k = \sqrt{k_j k_j}$, specifies the direction of propagation by the unit vector n_i . The magnitude k (the wave number) is complex for the attenuated waves. The wave function \mathcal{E} can be, of course, written in the form

$$\mathcal{E} = e^{-\text{Im}k \mathbf{n} \cdot \mathbf{x}} \exp[i(\text{Re}k \mathbf{n} \cdot \mathbf{x} - \omega t)], \quad (69)$$

which means that $\text{Im}k$ determines the attenuation and $c = \omega/\text{Re}k$ is the so-called phase speed of the monochromatic wave.

Substitution of the relations (68) in equations (24) and (25) and the subsequent elimination of E_{ij}^S, E^F yield the following algebraic set for V_i^S, V_i^F

$$\begin{aligned} \left[\left(\omega^2 + i \frac{\pi\omega}{\rho_0^S} \right) \delta_{ij} + \frac{\lambda^S}{\rho_0^S} k_i k_j + \frac{\mu^S}{\rho_0^S} (k^2 \delta_{ij} + k_i k_j) \right] V_j^S + \\ - \left(\frac{Q}{\rho_0^S} + i \frac{\pi\omega}{\rho_0^S} \right) V_0^F = 0, \\ \left(\frac{Q}{\rho_0^F} k_i k_j - i \frac{\pi\omega}{\rho_0^F} \right) V_0^S + \left[\left(\omega^2 + i \frac{\pi\omega}{\rho_0^F} \right) \delta_{ij} + \kappa k_i k_j \right] V_j^F = 0. \end{aligned} \quad (70)$$

This is, certainly, the eigenvalue problem. For any given frequency ω the determinant of this set yields the complex eigenvalues which determine phase speeds of propagation $c = \omega/\text{Re}k$ and attenuation $\text{Im}k$ of monochromatic waves. The corresponding eigenvectors determine modes of propagation. This problem has been thoroughly investigated.

REFERENCES

1. Albers B.: *Makroskopische Beschreibung von Adsorptions-Diffusions-Vorgängen in porösen Körpern*, Dissertation, TU-Berlin, Berlin, Logos-Verlag, 2000.
2. Albers B., Wilmanski K.: *On modeling acoustic waves in saturated poroelastic media*, J. Engng. Mech., **131**, 9 (2005) 974-985.
3. Albers B., Wilmanski K.: *Influence of coupling through porosity changes on the propagation of acoustic waves in linear poroelastic materials*, Arch. Mech., **58**, 4-5 (2006) 313-325.
4. Allard J. F.: *Propagation of Sound in Porous Media*, Elsevier Science, 1993.
5. Allen S. G., Stephenson P. C. L., Strange J. H.: *Morphology of porous media studied by nuclear magnetic resonance*, J. Chem. Phys., **106** (18) (1997) 7802-7809.
6. Arnold J.: *Mobile NMR for rock porosity and permeability*, PhD-Thesis, RWTH Aachen 2007.
7. Bachmat Y., Bear J.: *Macroscopic Modelling of Transport Phenomena in Porous Media, I. Continuum Approach*, Trans. Porous Media, **1**, (1986) 213-240.
8. Balzarini M., Brancolini A., Gossenbergh P.: *Permeability estimation from NMR diffusion measurements in reservoir rocks*, Magn. Res. Im. **16**, 5-6 (1998) 601-603.
9. Basser P. J., Mattiello J., LeBihan D.: *MR diffusion tensor spectroscopy and imaging*, Biophysical Journal, **66** (1994) 259-267.
10. Basser P. J., Derek K. J.: *Diffusion-tensor MRI: theory, experimental design and data analysis – a technical review*, NMR Biomed., **15** (2002) 456-467.
11. Basser P. J., Pajevic S.: *Statistical artifacts in diffusion tensor MRI (DT-MRI) caused by background noise*, Magnetic Resonance in Medicine **44**, (2000) 41-50.
12. Bear J.: *Dynamics of Fluids in Porous Media*, New York, Dover Publ. 1988 (American Elsevier, 1972).
13. Bear J., Bachmat Y.: *Introduction to Modeling of Transport Phenomena in Porous Media*, Dordrecht, Kluwer Academic Publishers 1991.
14. Bear J., Nitao J. J.: *Flow and Contaminant Transport in the Unsaturated Zone*, Dordrecht, Kluwer, 2005 (the first draft, private communication).
15. Bear J., Cheng A. H.-D.: *Modeling Groundwater Flow and Contaminant Transport (Theory and Applications of Transport in Porous Media)*, Dordrecht, Springer, 2010.

16. Beg M. F., Dickie R., Golds G., Younes L.: *Consistent realignment of 3D diffusion tensor MRI eigenvectors*, Medical Imaging 2007, Image Processing, J. P. W. Pluim, J. M. Reinhardt (eds.) 1-9.
17. Berryman J. G., Lumley D. E.: *Inverting ultrasonic data on solid/fluid mixtures for Biot-Gassmann parameters*, Proc. of the Second Int. Conf. on Mathematical and Numerical Aspects of Wave Propagation, Proc. SIAM, June 7-10, 1993, 57-68.
18. Biot M. A.: *Theory of propagation of elastic waves in a fluid-saturated porous solid. I. Low-Frequency Range*, J. Acoust. Soc. Am., **28**, (1956) 168-178.
19. Biot M. A.: *Theory of propagation of elastic waves in a fluid-saturated porous solid. II. Higher Frequency Range*, J. Acoust. Soc. Am., **28**, 2 (1956) 179-191.
20. Biot M. A.: *Generalized theory of acoustic propagation in porous dissipative media*, J. Acoust. Soc. Am., **34**, 5 (1962) 1254-1264.
21. Bloch F.: *Nuclear induction*, Phys. Review **70** (1946) 460-474.
22. Blümich B.: *Essential NMR for Scientists and Engineers*, Berlin, Springer, 2005.
23. Bolam A. C.: Packer K. J.: *A NMR characterisation of a banded sandstone*, Magn. Res. Im. **16**, 5-6 (1998) 609-611.
24. Boudreau B. P., Gardiner B. S., Johnson B. D.: *Rate of growth of isolated bubbles in sediments with a diagenetic source of methane*, Limnol Oceanogr. **46**, 3 (2001) 616-622.
25. Bourbie T., Coussy O., Zinszner B.: *Acoustics of Porous Media*, Paris, Editions Technip 1987.
26. Bowen R. M.: *Diffusion Models implied by the Theory of Mixtures*, in: Rational Thermodynamics (Second Edition), C. Truesdell (ed.), New York, Springer, 1984, 237-263.
27. Bubner N., Klein O., Philip P., J. Sprekels, Wilmanski K.: *A Transient Model for the Sublimation Growth of Silicon Carbide Single Crystals*, J. Crystal Growth, **205**, (1999) 294-304.
28. Bubner N., Klein O., Philip P., J. Sprekels, Wilmanski K.: *A Radiation- and Convection-driven Transient Heat Transfer During Sublimation Growth of Silicon Carbide Single Crystals*, J. Crystal Growth, **222**, (2001) 832-851.
29. Byrne H., Preziosi L.: *Modelling solid tumor growth using the theory of mixtures*, Mathematical Medicine and Biology, **20** (2003) 341-366.
30. Carman P. C.: *Fluid Flow Through a Granular Bed*, Trans. Inst. Chem. Engn. **15** (1937) 150-156.
31. Coussy O.: *Mechanics of Porous Media*, Chichester, John Wiley & Sons 1995.
32. Edwards J. C.: *Principles of NMR*, Process NMR Associates LLC, 87A Sand Pit Rd, Danbury CT 06810.

33. Epstein Ch.: *Introduction to magnetic resonance imaging for mathematicians*, Annales de l'Institut Fourier, Grenoble, **54**, 5 (2004) 1697-1716.
34. Epstein N.: *On Tortuosity and the Tortuosity Factor in Flow and Diffusion Through Porous Media*, Chem. Engn. Sci., **44**, 3 (1989) 777-779.
35. Erdmann B., Lang J., Matera S., Wilmanski K.: *Adaptive Linearly Implicit Methods for Linear Poroelastic Equations*, ZIP-Report 05 (2005).
36. Forchheimer P.: *Hydraulik* Leipzig/Berlin, Teubner, 1914.
37. *Fuel Cell Handbook* (Seventh Edition), EG&G Technical Services, Inc. Under Contract No. DE-AM26-99FT40575, Morgantown 2004.
38. Gregg S. J., Sing K. S. W.: *Adsorption, Surface Area and Porosity*, London, Academic Press, 1982.
39. Haber A., Haber-Pohlmeier S., Casanova F., Blümich B.: *Relaxation-relaxation experiments in natural porous media with a portable Halbach magnet*, RWTH Aachen, Report (2008).
40. Haber-Pohlmeier S., Bechtold M., Stapf S., Pholmeier A.: *Water flow monitored by tracer transport in natural porous media using MRI*, Jülich-Report (2009).
41. Hahn E., *Spin echoes*, Physical Review, **80** (1950)580-594.
42. Hasan K. M., Parker D. L., Alexander A. L.: *Magnetic resonance water self-diffusion tensor encoding optimization methods for full brain acquisition*, Image Anal Stereol, 21 (2002) 87-96.
43. Howard J. J.: *Quantitative estimates of porous media wettability from proton NMR measurements*, Magn. Res. Im. **16**, 5/6 (1998), 529-533.
44. Jaeger J. C., Cook N. G. W., Zimmerman R. W.: *Fundamentals of Rock Mechanics*, Malden, Blackwell Publ. 2007.
45. Johnson D. L., Plona T. J., Scala C.: *Tortuosity and acoustic slow waves*, Physical Review Letters, **49**, 25 (1982) 1840-1844.
46. Johnson D. L., Koplik J., Dashen R.: *Theory of dynamic permeability and tortuosity in fluid-saturated porous media*, J. Fluid Mech. **176** (1987) 379-402.
47. Kozeny J.: *Über kapillare Leitung des Wassers im Boden (Aufstieg, Versickerung und Anwendung auf die Bewässerung)*, Sber. Akad. Wiss., Wien **136** (Abt. IIa) (1927) 271-306.
48. Kubik J.: *A macroscopic description of geometrical pore structure of porous solids*. Int. J. Engn. Sci., **24**, 6 (1986) 971-980.
49. Kubik J., Cieszko M., Kaczmarek M.: *Podstawy Dynamiki Nasyconych Ośrodków Porowatych*, Warszawa, IPPT PAN, 2000.
50. Kubik J., Rybicki A., *Porosity of materials with a given permeability vector field (in Polish)*. Warsaw, IPPT Reports 72 (1979), 15–26.
51. Lai C. G., Wilmanski K.: *Surface Waves in Geomechanics: Direct and Inverse Modelling for Soils and Rocks*, WienNewYork, Springer 2005.

52. Landau L. D., Lifschitz E. M.; *Lehrbuch der theoretischen Physik. Band VI: Hydrodynamik*, Berlin, Akademie-Verlag, 1991.
53. Litster S., Djilali N.: *Two-phase transport in porous gas diffusion electrodes*, in: *Transport Phenomena in Fuel Cells*, B. Sunden, M. Faghri (eds.), Southampton, WIT Press 2005, 175-213.
54. Lopatnikov S. L., Gillespie, Jr., J. W.: *On the Mechanical Equilibrium of the Fluid-filled Poro-elastic Body*, in: *Promechanics – Biot Centennial (1905-2005)*, Abousleiman Y. N., Cheng A. H.d., Ulm F.-J. (eds.), Leiden, A. A. Balkema 2005, 85-90.
55. Mair R. W., Wong G. P., Hoffmann D., Hürlimann M. D., Patz S., Schwartz L. M., Walsworth R. L.: *Probing porous media with gas diffusion NMR*, *Physical Review Letters*, **83**, 16 (1999) 3324-3327.
56. Mair R. W., Hürlimann M. D., Sen P. N., Schwartz L. M., Patz S., Walsworth R. L.: *Tortuosity measurement and the effects of finite pulse widths on xenon gas diffusion NMR studies of porous media*, *Magnetic Resonance Imaging* (2000) 1-12.
57. Masutani Y., Aoki S., Abe O., Hayashi N., Otomo K.: *MR diffusion tensor imaging: recent advance and new techniques for diffusion tensor visualization*, *European Journal of Radiology* **46** (2003) 53-66.
58. Mavko G., Mukerji T., Dvorkin J.: *The Rock Physics Handbook*, Cambridge Univ. Press 1998.
59. McNab J. A.: *Diffusion pulse sequences*, Physics Group Meeting, January 15, 2006, 2-11.
60. Miyanaga M., Mizuhara N., Fujiwara S., Shimazu M., Nakahata H., Kawase T.: *Single Crystal Growth of AlN by Sublimation Method*, *SEI Technical Review* 63 (2006) 22-26.
61. Moldrup P., Olesen T., Komatsu T., Schjonning P., Rolston D. E.: *Tortuosity, diffusivity and permeability in the soil liquid and gaseous phases*, *Soil Sci. Soc. Am. J.*, **65** (2001) 613-623.
62. Moucheron P., Bertranda F., Kovall a G., Tocquera L., Rodtsa S., Rouxa J.-N., Corfdira A., Chevoir F.: *MRI investigation of granular interface rheology using a new cylinder shear apparatus*, *Magn. Res. Im.* **28**, 6 (2010) 910-918.
63. Newman J. N.: *Marine Hydrodynamics*, Cambridge, Massachusetts, MIT Press 1977.
64. Nield D. A., Bejan A.: *Convection in Porous Media (Third Edition)*, USA, Springer 2006.
65. Pajevic S., Pierpaoli C.: *Color schemes to represent the orientation of anisotropic tissues from diffusion tensor data: application to white matter fiber tract mapping in the human brain*, *Magn. Reson. Med.* **42**(3) (1999), 526-540.

66. Reppert Ph. M., Morgan F. D., Lesmes D. P., Jouniaux L.: *Frequency-dependent streaming potentials*, Journal of Colloid and Interface Science, **234** (2001) 194-203.
67. Rusakov D. A., Kullmann D. M.: *Geometric and viscous components of the tortuosity of the extracellular space in the brain*, Proc. Natl. Acad. Sci. USA, Neurobiology, **95** (1998) 8975-8990.
68. Santamarina J. C.: *Soils and Waves*, Chichester, John Wiley & Sons, LTD., 2001.
69. Saripalli K. P., Khaleel R., Serne J., Lindberg M., Parker K.: *Tortuosity of immiscible fluids in porous media based on phase interfacial areas: a new definition and its application to Handford's unsaturated media*, Seattle Annual Meeting, Geological Society of America Abstracts with Programs, **35**, 6 (2003) 482.
70. Sen P. N., Schwartz L. M.: *Surface relaxation and the long-time diffusion coefficient in porous media: periodic geometries*, Physical Review B, **49**, 1 (1994) 215-225.
71. Spanos T. J. T.: *The Thermodynamics of Porous Media*, Boca Raton, Chapman&Hall/CRC, 2001.
72. Stoll R. D.: *Sediment Acoustics*, New York, Springer, 1985.
73. Straley Ch., Rossini D., Vinegar H., Tutunjian P., Morriss Ch.: *Core analysis by low field NMR*, SCA-9404 (1994) 43-55.
74. Taylor W. D., Hsu E., Rama Krishnan K. R., MacFall J. R.: *Diffusion Tensor Imaging: Background, potential, and utility in psychiatric research*, Biol Psychiatry, **55** (2004) 201-207.
75. Torrey H. C.: *Bloch equations with diffusion terms*, Phys. Review **104** (1956) 563-565.
76. Truesdell C.: *Rational Thermodynamics (Second Edition)*, New York, Springer 1984.
77. Wang R., Pavlin T., Rosen M. S., Mair R. W., Cory D. G., Walsworth R. L.: *Xenon NMR measurements of permeability and tortuosity in reservoir rocks*, Magn. Res. Im. (2004) 1-9.
78. Watanabe Y., Nakashima Y.: *Two-dimensional random walk program for the calculation of the tortuosity of porous media*, Journal of Groundwater Hydrology, **43** (2001) 13-22.
79. Westphal H., Surholt I., Kiesel Ch., Thern H. F., Kruspe T.: *NMR measurements in carbonate rocks: problems and an approach to a solution*, Pure Appl. Geophys., **162** (2005) 549-570.
80. White J. E.: *Underground Sound. Application of Seismic Waves*, Amsterdam, Elsevier, 1983.
81. Wilhelm T., Wilmanski K.: *On the Onset of Flow Instabilities in Granular Media due to Porosity Inhomogeneities*, Int. J. Multiphase Flows **28** (2002) 1929-1944.

82. Wilmanski K.: *A Thermodynamic Model of Compressible Porous Materials with the Balance Equation of Porosity*, *Transp. Porous Media* **32** (1998) 21-47.
83. Wilmanski K.: *On a Homogeneous Adsorption in Porous Materials*, *ZAMM*, 81 (2001) 119-124.
84. Wilmanski K.: *Thermodynamics of Multicomponent Continua*, in: *Earthquake Thermodynamics and Phase Transitions in the Earth's Interior*, R. Teisseyre, E. Majewski (eds), San Diego, Academic Press, 2001, 567-656.
85. Wilmanski K.: *On Microstructural Tests for Poroelastic Materials and Corresponding Gassman-type Relations*, *Geotechnique*, **54**, 9 (2004) 593-603.
86. Wilmanski K.: *Tortuosity and objective relative accelerations in the theory of porous materials*, *Proc. Roy. Soc. A*, **461** (2005) 1533-1561.
87. Wilmanski K.: *A few remarks on Biot's model and linear acoustics of poroelastic saturated materials*, *Soil Dynamics & Earthquake Engineering*, **26**, 6-7 (2006) 509-536.
88. Wilmanski K.: *Continuum Thermodynamics. Part I: Foundations*, New Jersey, World Scientific 2008.
89. Wilmanski K.: *Diffusion and heat conduction in nonlinear thermoporoelastic media*, Chapter 9 of *Advances in the Mechanics of Inhomogeneous Media*, Cz. Wozniak, M. Kuczma, R. Switka, K. Wilmanski (eds.), Zielona Gora, University of Zielona Gora 2010, 123-148.
90. Yaramanci U.: *New Technologies in Groundwater Exploration. Surface Nuclear Magnetic Resonance*, *Geologica Acta*, 2, 2 (2004) 109-120.
91. Yaramanci U, Müller-Petke M.: *Surface nuclear magnetic resonance—A unique tool for hydrogeophysics*, *THE LEADING EDGE (Journal of the Society of Exploration Geophysicists)*, October (2009) 1240-1247.

DYFUZYJNOŚĆ, KRĘTNOŚĆ I TŁUMIENIE FAL W MATERIAŁACH POROWATYCH

Streszczenie

Praca zawiera zwięzłą prezentację konstrukcji liniowego modelu porospężystego i jego zastosowania w teorii fal akustycznych. Głównym celem tej prezentacji jest dyskusja parametrów materiałowych opisujących dyfuzję. Dotyczy to w szczególności dyfuzyjności i krętności. W Rozdziale 2 przytaczamy kilka przykładów ośrodków porowatych, w których dyfuzja odgrywa ważną rolę. Rozdział 3 zawiera zwięzły opis modelu dwuskładnikowego dla nasyconych ośrodków porowatych z dyfuzją. Uwypuklamy główne cechy takiego układu ze szczególnym uwzględnieniem ruchu względnego składników i zmian porowatości. Jako przypadek szczególny przedstawiane są równania modelu Biot. W rozdziale 4 dyskutujemy pojęcia dyfuzyjności,

przewodnictwa hydraulicznego i krętności. W szczególności wprowadzamy pojęcie tensora krętności. Rozdział 5 zawiera elementarne wiadomości dotyczące metody nuklearnego rezonansu magnetycznego w zastosowaniu do eksperymentów określających dyfuzyjność i krętność w różnych materiałach porowatych. Wreszcie rozdział 6 zawiera pewne zagadnienia związane z propagacją fal monochromatycznych, a w szczególności wpływu krętności na prędkości propagacji i tłumienie.

Praca wpłynęła do Redakcji